

Nucleation Processes in the Growth of hcp Titanium

J. C. A. Huang, R. R. Du, and C. P. Flynn

Department of Physics and the Materials Research Laboratory, University of Illinois at Urbana-Champaign, 1110 West Green Street, Urbana, Illinois 61801

(Received 29 May 1990)

Six distinct orientations of hcp titanium have been grown as high-quality single crystals by molecular-beam epitaxy. The substrates were freshly grown bcc metals on sapphire. We identify four different nucleation mechanisms that compete to select the eventual crystal orientation. In one novel case, the growth of tilted Ti(10 $\bar{1}$ 2) is identified with nucleation at step edges rather than on terraces of the stepped Ta(211) substrate.

PACS numbers: 68.55.Bd, 68.35.-p, 68.55.Nq

The way epitaxial crystals nucleate from molecular beams is much less well understood than their subsequent heteroepitaxial growth. For example, the Frank-Van der Merwe (layer by layer<sup>1</sup>), Volmer-Weber (island<sup>2</sup>), and Stanski-Krastanov (islands bridged by monolayer<sup>3</sup>) growth modes are all observed in molecular-beam epitaxy<sup>4</sup> (MBE), and are reproduced by theoretical modeling.<sup>5,6</sup> There is a firm understanding of the energetic factors that can cause each of them to be preferred in the growth of systems near equilibrium. Factors such as symmetry and lattice match, that are relevant instead to the nucleation of a heteroepitaxial film, have also long been recognized, and have been identified in particular cases as critical determinants of the eventual epilayer orientation.<sup>7</sup> At present, however, there exists only an extremely limited ability to predict what epilayer orientation is preferred in specific cases.

In the present work we report unprecedented epitaxial control in which a single material, hcp Ti, is grown as a high-quality single crystal in six distinct orientations on substrates that are chemically similar but different in geometry. Four different nucleation criteria appear to operate in the six cases. One of these permits an identification of three-dimensional (3D) nucleation that occurs specifically at surface step edges rather than on surface terraces. We assess the degree to which any of these results is predictable at the present time.

By careful attention to growth conditions we have been able to synthesize Ti films in the six orientations indicated in Fig. 1(a). These include the (0001) basal plane, the (11 $\bar{2}$ 0) slip plane perpendicular to it, and a sheaf of planes based on (10 $\bar{l}$ l), with  $l=0,1,2,3$ . We emphasize that in each orientation the surface grows atomically flat as seen by reflection high-energy electron diffraction (RHEED). Examples are provided in Fig. 2 to document the quality of the final surfaces. The (10 $\bar{1}$ 2) and (0001) surfaces, with poor fit to their respective substrates, exhibited spotty RHEED patterns for the initial coverage, which smoothed to the observed streaks (Fig. 2) after 50 Å; the remaining four surfaces were fairly smooth from the beginning, but nevertheless still

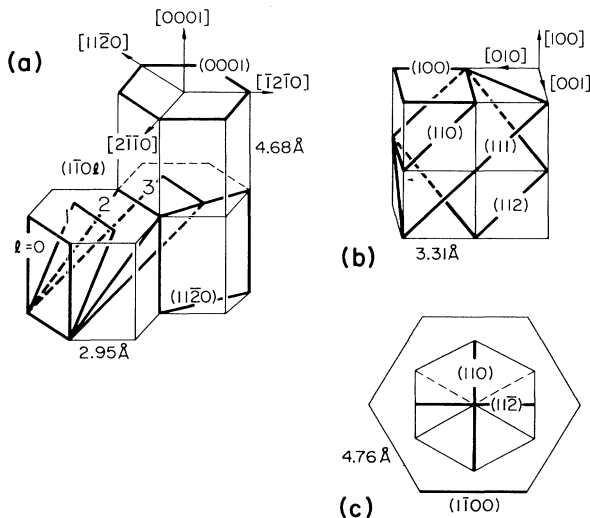


FIG. 1. (a) The six growth planes of hcp Ti studied here and (b) the four planes of bcc Ta. (c) View from above a hexagonal prism supporting a cube with one body diagonal vertical. These are the relative orientations of the Al<sub>2</sub>O<sub>3</sub> and Ta lattices discussed in the text.

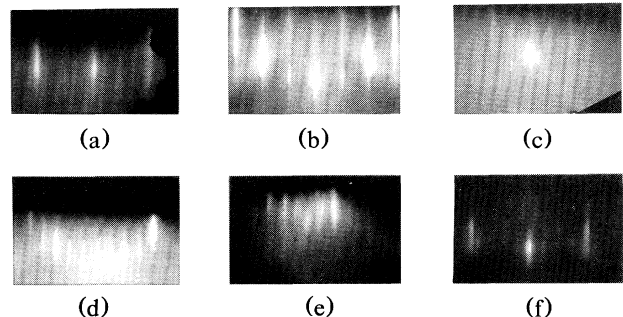


FIG. 2. RHEED patterns of Ti films grown on Ta or Mo and studied here: (a) Ti(0001) along [11 $\bar{2}$ 0]; (b) Ti(10 $\bar{1}$ 0) along [11 $\bar{2}$ 0]; (c) Ti(10 $\bar{1}$ 1) along [11 $\bar{2}$ 0]; (d) Ti(10 $\bar{1}$ 3) along [11 $\bar{2}$ 0]; (e) Ti(10 $\bar{1}$ 2) along [11 $\bar{2}$ 0] with angled streaks corresponding to (10 $\bar{1}$ 3); (f) Ti(11 $\bar{2}$ 0) along [1 $\bar{1}$ 00].

showed some improvement with thickness. X-ray studies verified the crystal orientations and revealed high-quality bulk material with structural coherence  $\sim 500$  Å and mosaic spread  $\leq 0.35^\circ$  in all cases except Ti(10 $\bar{1}2$ ). No such epitaxial control has been achieved previously. Four planes of bcc Nb (Ta) is the most grown to date;<sup>8</sup> hexagonal crystals have been thought more difficult, and have been grown selectively in three epitaxial orientations only by homoepitaxy on bulk crystals.<sup>9</sup>

To grow these Ti surfaces we employed the synthesis route via epitaxial grade sapphire first explored by Durbin, Cunningham, and Flynn.<sup>6</sup> Ta or Mo was grown on the  $\alpha$ -Al<sub>2</sub>O<sub>3</sub> at about 900°C and the Ti crystals subsequently grown on the fresh bcc metal at about 400°C. Typical molecular-beam fluxes gave growth rates of about 0.5 Å/sec. These conditions are consistent with the requirements of step flow growth,<sup>10</sup> with resulting surface perfection evident in Fig. 2. A Perkin Elmer 400 MBE chamber equipped with two *e*-beam sources<sup>11</sup> was employed for this work. With pressures in the 10<sup>10</sup>-torr range during growth it is extremely unlikely that residual gases played a role in determining the epilayer orientation. The four bcc planes used here as templates for Ti nucleation were (100), (00 $\bar{1}$ ), ( $\bar{1}11$ ), and (211), respectively, grown on  $\alpha$ -Al<sub>2</sub>O<sub>3</sub> ( $\bar{1}102$ ), (11 $\bar{2}0$ ), (0001), and ( $\bar{1}100$ ). Planes of these types are shown in Fig. 1(b) for the convenience of the reader.

Table I lists the six Ti orientations that nucleate on specific bcc surfaces, together with the underlying  $\alpha$ -Al<sub>2</sub>O<sub>3</sub> substrate cut. Chemical factors are minimized by confining the substrates to Ta and, in once case, Mo. Data of this extent provide a substantial overview of what planes can and what cannot nucleate on each other. We believe that systematic explorations of this type provide a valuable approach to the problem of understanding nucleation on surfaces. The evidence for hcp Ti on these bcc metals is examined in what follows.

Three of the observed Ti orientations appear to have straightforward geometrical explanations. When Ta( $\bar{1}11$ ) and Ti(0001) grow successively on  $\alpha$ -Al<sub>2</sub>O<sub>3</sub>(0001) the selected one of four Ta orientations and one of six Ti orientations both preserve threefold surface symmetry without other significant matching, for exam-

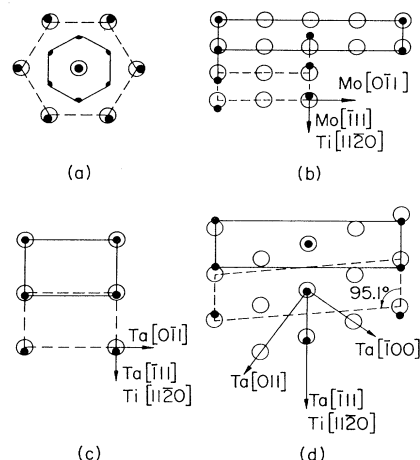


FIG. 3. Surface nets for four cases of good fit, with open circles for bcc atoms and solid circles for hcp atoms: (a) Ti(0001) on Ta( $\bar{1}11$ ); (b) Ti(10 $\bar{1}3$ ) on Mo(211); (c) Ti(10 $\bar{1}0$ ) on Ta(211); (d) Ti(10 $\bar{1}1$ ) on Ta(01 $\bar{1}$ ). In (a) the inner hexagon represents the underlying  $\alpha$ -Al<sub>2</sub>O<sub>3</sub> lattice.

ple in lattice spacing. It can hardly be questioned in either case that the threefold local structure of terrace sites available during nucleation create correctly oriented nuclei that subsequently grow together. Equally plausible, if different, are the two further cases of Ti epitaxy on the "magic" (211) terraces of Mo and Ta, both grown on  $\alpha$ -Al<sub>2</sub>O<sub>3</sub>( $\bar{1}100$ ). In each case the epilayer and substrate both have tetragonal surface nets that exhibit a good mutual 2D match. The repeat lengths are 8.98 Å  $\times$  2.95 Å for Ti(10 $\bar{1}3$ ) on Mo(211) with repeats of 8.91 Å  $\times$  2.73 Å; the comparable numbers are 4.68 Å  $\times$  2.95 Å for Ti(10 $\bar{1}0$ ), and 4.68 Å  $\times$  2.87 Å for Ta(211). Thus the nucleation process that selects the eventual orientations for these two cases can be attributed to the availability of good 2D registry. Sketches of the three pairs of surface nets discussed thus far are given in Figs. 3(a)–3(c).

A two-dimensional fit also appears as the main factor in Ti(10 $\bar{1}1$ ) nucleation on Ta(01 $\bar{1}$ ). This Ta orientation grows well on  $\alpha$ -Al<sub>2</sub>O<sub>3</sub>(11 $\bar{2}0$ ) under clean conditions and

TABLE I. Epitaxial relationships for Ti/bcc/Al<sub>2</sub>O<sub>3</sub>, and x-ray Bragg width  $\delta 2\theta$  and rocking-curve width  $w$  for Ti films.

Substrate	bcc	Ti	$\delta 2\theta$ (deg)	$w$ (deg)	$t$ (Å)
Al <sub>2</sub> O <sub>3</sub> (0001)	Ta( $\bar{1}11$ )	Ti(0001)	0.18	0.34	2100
Al <sub>2</sub> O <sub>3</sub> ( $\bar{1}102$ )	Ta(100)	Ti(11 $\bar{2}0$ )	0.20	0.32	1050
Al <sub>2</sub> O <sub>3</sub> ( $\bar{1}100$ )	Ta(211)	Ti(10 $\bar{1}0$ )	0.15	0.28	1280
Al <sub>2</sub> O <sub>3</sub> (11 $\bar{2}0$ )	Ta(01 $\bar{1}$ )	Ti(10 $\bar{1}1$ )	0.20	0.35	1020
		Tilted			
Al <sub>2</sub> O <sub>3</sub> ( $\bar{1}100$ ) <sup>a</sup>	Ta(211)	Ti(10 $\bar{1}2$ )	0.32	0.70	850
Al <sub>2</sub> O <sub>3</sub> ( $\bar{1}100$ )	Mo(211)	Ti(10 $\bar{1}3$ )	0.20	0.35	960

<sup>a</sup>Al<sub>2</sub>O<sub>3</sub>( $\bar{1}100$ ) substrate, miscut by 1.4° along Al<sub>2</sub>O<sub>3</sub>[11 $\bar{2}0$ ].

on a variety of other surfaces as vacuum conditions deteriorate. Figure 3(d) shows how a cell  $2.87 \text{ \AA} \times 10.85 \text{ \AA}$  with an included angle of  $95.1^\circ$  for  $\text{Ta}(01\bar{1})$  fits closely with the  $\text{Ti}(10\bar{1}1)$  cell of size  $2.95 \text{ \AA} \times 10.66 \text{ \AA}$  with an angle of  $90^\circ$ . The three systems of Figs. 3(b)–3(d) thus appear to be selected for 2D fit. Note in addition that each has a  $[\bar{1}11]$  azimuth parallel to a  $[11\bar{2}0]$  azimuth, similar to the Kurdjumov-Sachs<sup>6,12</sup> (KS) relationship for the hcp case, and with a remarkably good fit ( $2.87 \text{ \AA}$  vs.  $2.95 \text{ \AA}$  for Ta or  $2.73 \text{ \AA}$  for Mo) along the common axis. The KS relationship is important also in the polymorphic transformation between  $\alpha$ -Ti (hcp) and  $\beta$ -Ti (bcc).<sup>13</sup> In contrast neither the KS relationship nor lattice fit enters into the case of Fig. 3(a), which appears to involve only site symmetry.

In the fifth and perhaps most interesting process studied here nucleation again takes place on  $\text{Ta}(211)$ . This surface nucleates different Ti orientations depending on the substrate miscut and the growth temperature. Sapphire surfaces cut within  $0.4^\circ$  of  $(\bar{1}100)$ , when overgrown with high-quality  $\text{Ta}(211)$ , nucleate  $\text{Ti}(10\bar{1}0)$  because the two surface nets fit well, as described above. Quite different behavior is observed when the  $\alpha$ - $\text{Al}_2\text{O}_3$  is miscut by  $1.4^\circ$  along  $[11\bar{2}0]$ . Then, at 400 and  $450^\circ\text{C}$ ,  $\text{Ti}(10\bar{1}2)$  grows tilted by  $10.7^\circ$  along the  $[01\bar{1}]$  azimuth of  $\text{Ta}(211)$ , whereas the  $\text{Ti}(10\bar{1}0)$  growth persists unchanged at 350, 300, and  $250^\circ\text{C}$ . It persists at higher temperatures also when the miscut is  $1^\circ$  along the  $\alpha$ - $\text{Al}_2\text{O}_3$   $[0001]$  azimuth instead. Both variants preserve the KS relationship. The interpretation of these important observations seems quite clear. The vicinal  $\alpha$ - $\text{Al}_2\text{O}_3$  surfaces remain largely  $(\bar{1}100)$  terraces with a  $\text{Ta}(211)$  overlayer (Fig. 4). For low temperatures, and consequently short diffusion lengths, nucleation is confined to the terraces and  $\text{Ti}(10\bar{1}0)$  grows. With increasing temperature and miscut, however, the Ti can sample the step edges that separate individual terraces. The conclusion appears straightforward that  $\text{Ti}(10\bar{1}2)$  is nucleated at the step ledges caused by miscut along  $[11\bar{2}0]$ . These we take to have  $\alpha$ - $\text{Al}_2\text{O}_3$   $(11\bar{2}0)$  geometry. We return below to discuss 3D aspects of this process. No clear-cut demonstration of epitaxial orientations nucleated solely at step edges has previously been reported. It is particularly noteworthy that the resulting Ti single crystals are of high quality with coherence lengths  $\geq 500 \text{ \AA}$ .

We finally discuss the case of  $\text{Ta}(100)$ . On  $\alpha$ - $\text{Al}_2\text{O}_3$   $(\bar{1}102)$  this surface grows tilted by about  $2.9^\circ$  along the  $[1\bar{1}01]$  azimuth.<sup>14,15</sup> Were  $\alpha$ - $\text{Al}_2\text{O}_3$  ideally hcp, the four observed bcc orientations  $(100)$ ,  $(01\bar{1})$ ,  $(\bar{1}11)$ , and  $(211)$  with their respective substrates of  $(\bar{1}102)$ ,  $(11\bar{2}0)$ ,  $(0001)$ , and  $(\bar{1}100)$   $\alpha$ - $\text{Al}_2\text{O}_3$  would correspond to the fixed relative orientation of the bcc and hcp lattice shown in Fig. 1(c). This could possibly arise from chemical reactions at the interface that prefer a specific bcc orientation relative to the  $\alpha$ - $\text{Al}_2\text{O}_3$  oxygens. For the actual  $c/a$  ratio of  $\alpha$ - $\text{Al}_2\text{O}_3$  the  $(\bar{1}102)$  plane is tilted by  $2.9^\circ$  relative to the three orthogonal axes; this is

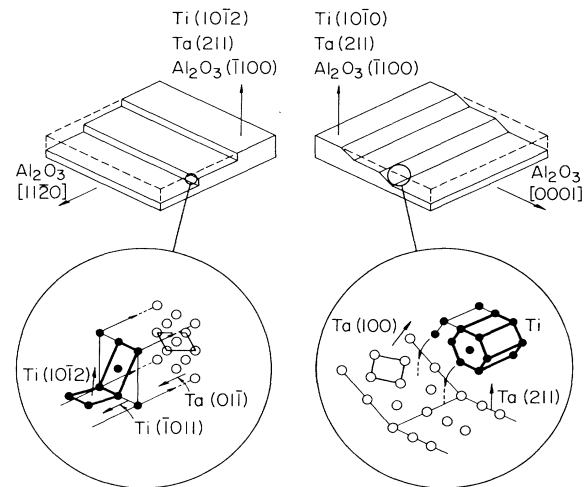


FIG. 4. Sketch showing Ta and Ti grown successively on miscut  $\alpha$ - $\text{Al}_2\text{O}_3$   $(\bar{1}100)$ . The insets show how good 3D registry is achieved at the step edges for  $\text{Ti}(10\bar{1}0)$  on  $\text{Ta}(211)$  with the miscut along  $\alpha$ - $\text{Al}_2\text{O}_3$   $[0001]$ , and for  $\text{Ti}(10\bar{1}2)$  grown tilted on  $\text{Ta}(211)$  for  $\alpha$ - $\text{Al}_2\text{O}_3$  miscut along  $[11\bar{2}0]$ .

consistent with the measured  $2.9^\circ$  tilt of the nucleated bcc  $(100)$ . We observe that on this tilted  $\text{Ta}(100)$  surface,  $\text{Ti}(11\bar{2}0)$  grows tilted back by  $3^\circ$  almost parallel to the underlying  $\alpha$ - $\text{Al}_2\text{O}_3$   $(\bar{1}102)$  planes. In this connection we note that  $\text{Ti}(11\bar{2}0)$  and  $(10\bar{1}0)$  are  $30^\circ$  apart whereas their  $\text{Ta}(100)$  and  $(211)$  substrates are  $35.3^\circ$  apart. Thus, if Ti is grown on  $\alpha$ - $\text{Al}_2\text{O}_3$   $(\bar{1}102)$  with  $(\bar{1}100)$  steps, reasonably good registry for both  $(100)$  and  $(211)$  is assured, with the  $3^\circ$  tilt representing some average between the two planes to accommodate the  $5.3^\circ$  misfit. This fit is further preferred by the identical spacings of Ti  $[0001]$  and Ta  $[01\bar{1}]$  at  $4.68 \text{ \AA}$  along the length of a step edge. It thus appears that factors involving 3D registry<sup>15</sup> may be relevant to the nucleation of the  $\text{Ti}(11\bar{2}0)$ .

In connection with 3D matching it is now worth noting that related factors enter into the step-edge nucleation of  $\text{Ti}(10\bar{1}2)$ , described above.  $\alpha$ - $\text{Al}_2\text{O}_3$   $(\bar{1}100)$  misoriented along  $[0001]$  consists of  $(\bar{1}100)$  terraces probably with  $(\bar{1}102)$  step edges<sup>16</sup> (Fig. 4), on which  $\text{Ta}(211)$  and  $\text{Ta}(100)$  grow, respectively.  $\text{Ti}(10\bar{1}0)$  growing on the Ta terraces then fits well with  $\text{Ti}(11\bar{2}0)$  on the  $\text{Ta}(100)$  step edges because of the 3D relationship mentioned above. When  $\alpha$ - $\text{Al}_2\text{O}_3$  is miscut along  $(11\bar{2}0)$ , however, the step edges of the vicinal surface may resemble  $(11\bar{2}0)$  planes.  $\text{Ta}(211)$  and  $\text{Ta}(01\bar{1})$  then grow on the terraces and step edges, respectively (Fig. 4). On the  $\text{Ta}(01\bar{1})$  step edges, Ti nucleates in the  $(\bar{1}011)$  orientation, as reported above. This plane is no longer compatible with subsequent  $(10\bar{1}0)$  terraces. Instead, as illustrated in Fig. 4, this orientation is consistent with the observed  $\text{Ti}(10\bar{1}2)$  on the  $\text{Ta}(211)$  terraces, and with a predicted tilt of  $10.3^\circ$  that compares well with the observed  $10.7^\circ$  tilt. It remains for future work to characterize the actual step-

edge structure in detail, and to provide an understanding of the way that Ta step edges carry the full  $(01\bar{1})$  template. The relationships identified here nevertheless offer a promising if, as yet, speculative explanation of the Ti orientation actually observed.

In summary, high-quality hcp Ti has been nucleated and grown epitaxially in six low-index orientations on fresh bcc surfaces of Ta (Mo) on sapphire. Four orientations may be explained by good match of the two surface nets, of which three involve 2D registry and one involves symmetry alone. The further case of nucleation on tilted Ta(100) gives tilted Ti(11 $\bar{2}$ 0) that appears to be a compromise between fits on the two Ta planes that form the terraces and step edges. Its sensitivity to temperature and miscut identify the sixth case with a 3D nucleation event that takes place specifically at step edges, explored here for the first time. We conclude that nucleation involves diverse mechanisms, even when chemical factors are held relatively unchanged. Even in retrospect it is not clear that the cases that involve 2D matching could be predicted by examination of the available low-index meshes. Nor is there a clear explanation why the threefold surfaces provide such a strong symmetry template during nucleation. The two cases where 3D structure enters are evidently still more complex. These geometrical facts are placed in perspective by the present research because a considerable number of related cases are studied together.

We thank F. Tsui for helpful discussions. This work was supported in part by NSF Grant No. DMR-88-20888.

<sup>1</sup>F. C. Frank and J. H. Van der Merwe, Proc. Roy. Soc. London A **198**, 216 (1948).

<sup>2</sup>M. Volmer and A. Weber, Z. Phys. Chem. **119**, 277 (1926).

<sup>3</sup>J. N. Stranski and L. Krastanov, Ber. Akad. Wiss. Wien **146**, 797 (1938).

<sup>4</sup>See, e.g., A. Zangwill, in *Physics at Surfaces* (Cambridge Univ. Press, Cambridge, 1988), p. 428; R. Kern, G. LeLay, and G. Metois, in *Current Topics in Materials Science*, edited by E. Kalids (North-Holland, Amsterdam, 1979), Vol. 3, Chap. 3.

<sup>5</sup>E. Bauer, Z. Krist. **110**, 372 (1958).

<sup>6</sup>E. Bauer, Appl. Surf. Sci. **11**, 479 (1982).

<sup>7</sup>See, e.g., M. A. Herman and H. Siffer, in *Molecular Beam Epitaxy* (Springer-Verlag, Berlin, 1988), p. 218.

<sup>8</sup>S. M. Durbin, J. E. Cunningham, and C. P. Flynn, J. Phys. F **12**, L75 (1982).

<sup>9</sup>R. Du, F. Tsui, and C. P. Flynn, Phys. Rev. B **38**, 2941 (1988).

<sup>10</sup>C. P. Flynn, J. Phys. F **18**, L195 (1988).

<sup>11</sup>S. M. Durbin, Ph.D. thesis, University of Illinois, 1983 (unpublished), p. 33.

<sup>12</sup>See Zangwill (Ref. 4), p. 422.

<sup>13</sup>See, e.g., A. Kelly and G. W. Groves, *Crystallography and Crystal Defects* (Longman, London, 1970), p. 319.

<sup>14</sup>D. B. McWhan, in *Layered Structures, Epitaxy and Interfaces*, edited by J. M. Gibson and L. R. Dawson, MRS Symposium Proceedings No. 37 (Materials Research Society, Pittsburgh, 1985), p. 493.

<sup>15</sup>J. H. Claassen, S. A. Wolf, S. B. Qadry, and L. D. Jones, J. Cryst. Growth **81**, 557 (1987).

<sup>16</sup>( $\bar{1}102$ ) is the cleavage plane of sapphire. See, e.g., C. C. Chang, J. Vac. Sci. Technol. **8**, 500 (1971).

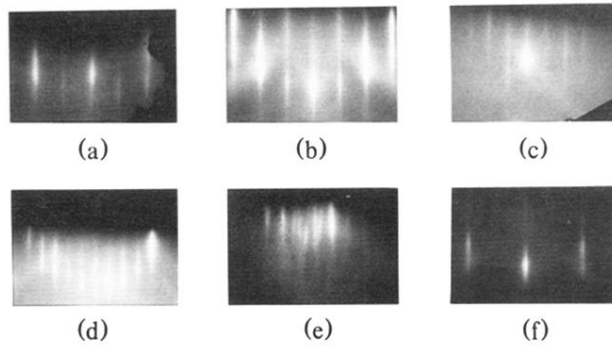


FIG. 2. RHEED patterns of Ti films grown on Ta or Mo and studied here: (a) Ti(0001) along  $[11\bar{2}0]$ ; (b) Ti( $10\bar{1}0$ ) along  $[11\bar{2}0]$ ; (c) Ti( $10\bar{1}1$ ) along  $[11\bar{2}0]$ ; (d) Ti( $10\bar{1}3$ ) along  $[11\bar{2}0]$ ; (e) Ti( $10\bar{1}2$ ) along  $[11\bar{2}0]$  with angled streaks corresponding to ( $10\bar{1}3$ ); (f) Ti( $11\bar{2}0$ ) along  $[1\bar{1}00]$ .